

# Phase structure of a $U(1)_L \otimes U(1)_R$ symmetric Yukawa model

Lee Lin, István Montvay and Hartmut Wittig

*Deutsches Elektronen-Synchrotron DESY, W-2000 Hamburg 52, FRG*

Received 19 March 1991; revised manuscript received 24 May 1991

The phase structure of the  $U(1)_L \otimes U(1)_R$  symmetric lattice Yukawa model with a mirror pair of fermion fields is explored by numerical Monte Carlo simulation. Its implications on the continuum physics are discussed.

## 1. Introduction

Simple prototype scalar-fermion models on the lattice, which have some qualitative features in common with the Higgs-Yukawa sector of the standard model, are the chiral  $SU(2)_L \otimes SU(2)_R$  symmetric [1] and  $U(1)_L \otimes U(1)_R$  symmetric [2-4] models with mirror pairs of fermion fields. In previous papers the  $U(1)_L \otimes U(1)_R$  model was investigated in the vicinity of the gaussian fixed point at zero couplings both in the symmetric and broken phases by applying lattice perturbation theory, hopping parameter expansion and numerical simulation techniques [2-5]. In order to explore the regions of very strong bare Yukawa couplings, far away from the gaussian fixed point, the knowledge of the detailed phase structure is necessary. In recent studies of several different lattice scalar-fermion models a rich phase structure was revealed [6-13], more or less independently of the number of scalar and fermion field components, the global symmetry group and the lattice formulation. (For recent reviews see also ref. [14]).

In this letter we investigate in detail the phase structure of the  $U(1)_L \otimes U(1)_R$  symmetric Yukawa model with a mirror pair of fermion fields. Our aim is to prepare future non-perturbative studies in the region of very strong bare Yukawa couplings, and to compare the qualitative features of the phase structure to other, recently investigated lattice Yukawa models. There are many interesting questions about the qualitative features of strongly interacting scalar-fermion models, which can be studied in a non-per-

turbative lattice formulation. If there is no non-trivial fixed point, the continuum limit is trivial, and there is an upper bound on the renormalized scalar self-coupling at any fixed values of the Yukawa couplings. The lower bound arises from the so-called "vacuum stability" requirement, which is usually formulated in the framework of perturbation theory. (See, for instance, ref. [15].) On the lattice the boundary corresponding to vanishing bare scalar self-coupling yields this "vacuum stability bound". (See ref. [4] for a detailed discussion on this matter.) Data about the allowed region between the lower and upper bounds on the renormalized quartic scalar coupling can be obtained by numerical Monte Carlo simulations. The first results on a small lattice ( $4^3 \times 8$ ), and the phase structure in the vicinity of the gaussian fixed point and in some other limiting cases were already reported in ref. [5].

The notations used in this paper are the same as in refs. [2-4]. For instance, the action of the  $U(1)_L \otimes U(1)_R$  model is given by eq. (1) in ref. [3]. For the definition of the renormalized quantities in the symmetric and broken phases see, respectively, ref. [3] and ref. [4]. In the next section we present the phase structure of our model in different limiting cases and at intermediate values of the Yukawa couplings. Tuning in the broken phase is discussed in section 3. Then we will conclude this report in the last section by some discussions on the continuum limit.

## 2. Phase structure

We explore the phase structure of our model both analytically and numerically (on  $4^3 \times 8$  and  $4^3 \times 16$  lattices). The bare scalar self-coupling  $\lambda$  is fixed to be infinite (the so-called Ising limit). This is not a serious restriction, because our previous experience tells that the qualitative features are independent of  $\lambda$ .

As a function of the fermion hopping parameter ( $K$ ) and bare Yukawa coupling of fermion ( $G_\psi$ ) and mirror fermion ( $G_\chi$ ) there are four limiting cases, in which the model reduces to the pure two-component  $\phi^4$  model. Namely at  $K=0, \infty$  while  $|G_\psi|$  and  $|G_\chi|$  are finite, and  $|G_\psi|=|G_\chi|=0, \infty$  at finite values of  $K$ . In these four limits, as a function of the scalar hopping parameter  $\kappa$ , at  $\kappa=\kappa_0 \simeq 0.15$ , the model has a second order phase transition from the ferromagnetic phase (denoted by FM phase) to the symmetric or paramagnetic phase (denoted by PM phase). In the FM phase the scalar field  $\phi_x$  has a non-zero vacuum expectation value. At negative scalar hopping parameter  $\kappa=-\kappa_0 \simeq -0.15$  there is another second order phase transition from the PM phase to the anti-ferromagnetic phase (denoted by AFM phase), where the *staggered scalar field*

$$\hat{\phi}_x \equiv (-1)^{x_1+x_2+x_3+x_4} \phi_x \quad (1)$$

has a non-zero vacuum expectation value. In the FM and AFM phases, the  $U(1)_L \otimes U(1)_R$  chiral symmetry is spontaneously broken to a vector-like  $U(1)$  symmetry by the vacuum expectation values of the scalar and staggered scalar fields, respectively.

In the very weak and strong Yukawa-coupling limits, we carry out small- and large- $G$  expansions of the fermion determinant in the effective bosonic action to next to leading order and find

$$\kappa_c = \kappa_0 - N_f K^2 (G_\psi^2 - 2G_\psi G_\chi + G_\chi^2) \quad (2)$$

for weak Yukawa couplings, and

$$\kappa_c = \kappa_0 - 2N_f K^2 \left( \frac{1}{G_\psi^2} - \frac{2}{G_\psi G_\chi} + \frac{1}{G_\chi^2} \right)$$

at strong couplings, where  $N_f$  is the number of fermion-mirror pairs. ( $N_f=2$  in our case.)

Since in our model there are two mass scales (the scalar and fermion masses), the continuum limit should be defined such that both masses go to zero

while their ratio is kept constant. Therefore we also have to study the critical surface on which the fermion mass vanishes. The value of  $K$  where this critical surface passes through is denoted by  $K_c$ . At  $G_\psi=G_\chi=0$ , we have  $K_c=\frac{1}{8}$ , since the fermions are free. At small  $|G_\psi|$  and  $|G_\chi|$ , one can estimate  $K_c$  by using one-loop bare perturbation theory (see ref. [3]). We find, qualitatively,

$$\begin{aligned} K_c &\searrow \text{ as } |G_\psi G_\chi| \nearrow & \text{ if } G_\psi G_\chi \geq 0, \\ K_c &\nearrow \text{ as } |G_\psi G_\chi| \nearrow & \text{ if } G_\psi G_\chi < 0. \end{aligned}$$

This qualitative behaviour has been seen in our numerical simulations. From the above analysis, we know the phase structure near the gaussian fixed point (see fig. 1 in ref. [5]).

At intermediate values of the Yukawa couplings we need to rely on Monte Carlo simulations, to explore the phase structure. The phase boundaries were always searched in the  $(K, \kappa)$ -plane at some fixed values of the Yukawa couplings  $G_\psi$  and  $G_\chi$ . The algorithm we use is the unbiased hybrid Monte Carlo method [16]. As discussed in ref. [3], this requires the flavour doubling of the fermion spectrum (i.e.:  $N_f=2$ ). The number of leapfrog steps per trajectory was chosen randomly between 3 and 10. The step size is tuned such that the acceptance rate is around 75%. The necessary inversions of the fermion matrix were done by the conjugate gradient iteration until the residuum was smaller than  $10^{-8}$  times the length squared of the input vector. We chose periodic boundary conditions along the spatial directions. In the time direction periodic boundary conditions were taken for the scalar field and antiperiodic ones for the fermions.

We find that when  $|G_\psi|$  and  $|G_\chi|$  are weak, as we move down along the  $\kappa$ -direction at any  $K$  value, the system will go from the FM phase to the PM and then to the AFM phase. We also find that the critical line separating the FM and PM phases bends down as we go to larger  $K$  values, and then it goes up gradually and levels off as  $K$  goes to infinity. The same is true for the critical line between PM and AFM phases. However, the curvature of bending of this lower critical line is smaller than that of the upper one. We explore this matter in some detail at  $(G_\psi=0.1, G_\chi=-0.3)$ . The results are plotted in fig. 1. We tune  $\kappa$  to find the points in the PM phase where either the sca-

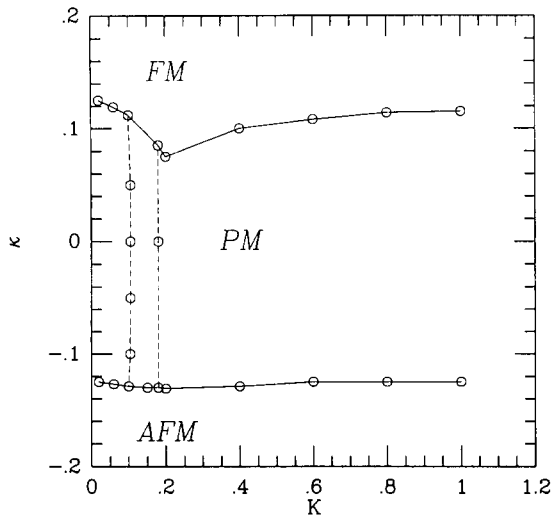


Fig. 1. The phase structure of our model at  $\lambda=\infty$  and  $(G_\psi=0.1, G_\chi=-0.3)$  is shown, as measured by Monte Carlo simulations on the  $4^3 \times 8$  lattice. We use open circles to represent points in the PM phase. Along the full lines the scalar mass is  $m_R \approx 1$ . On the almost vertical dashed lines the fermion mass is  $|\mu_R| \approx 1$ . The FM-PM and PM-AFM phase boundaries are near the full lines. No FI phase is found here.

lar mass or the staggered scalar mass is around 1.0 on our  $4^3 \times 8$  lattice. (The staggered scalar mass is defined in the same way as the scalar mass, only the scalar field  $\phi_x$  is replaced everywhere by the staggered scalar field  $\hat{\phi}_x$  in (1).) The true critical line is in the vicinity of these points. We also look for points where the fermion mass is around 1.0. In the figure the corresponding points are connected by full lines (for the scalar) and dashed lines (for the fermion), in order to give some idea about the position of the critical lines in the  $(K, \kappa)$ -plane. As shown in the figure, when  $K \geq 0.3$ , the two critical lines with zero scalar mass do go up and then level off. For the critical line with zero fermion mass we find  $K_c \approx 0.125$  here. It is interesting to note that this critical line is not a phase boundary: there is the same phase on both sides, only the sign of the renormalized fermion mass is opposite. (Note that this sign has no physical significance, since it can be transformed away by a  $\gamma_5$ -transformation [3].)

As we go to larger values of  $|G_\psi|$  and  $|G_\chi|$ , a new phase with both ferromagnetic and antiferromagnetic long-range order (i.e. non-zero vacuum expectation values of both  $\phi_x$  and  $\hat{\phi}_x$ ) shows up in the Monte Carlo simulations. This is because the FM-

PM boundary catches the PM-AFM boundary at negative  $\kappa$  and crosses it. We call this ferrimagnetic (FI) phase. However, for instance at  $(G_\psi=0.1, G_\chi=-1.0)$ , the width of this FI phase in the  $\kappa$ -direction is still quite narrow. The results are shown in fig. 2. As expected, when we go to larger  $K$  values the FI phase disappears, because the FM-PM boundary moves again above the PM-AFM boundary, and the phase structure is again like that of the pure scalar model: the system goes from the FM to PM and then to the AFM phase, if one goes from positive to negative  $\kappa$  values at fixed  $K$ . A similar phase structure with FM, PM, AFM and FI phases was observed earlier in other scalar-fermion models on the lattice [6-13].

Our data also show that there is a point in the  $(K, \kappa)$ -plane around which the FM, PM, FI and AFM phases coexist. A consequence of such a point (often called in the literature "point A") is that in this region both the scalar mass and the staggered scalar mass are small. This is the explanation of the "unexpected" behaviour of the scalar propagator as a func-

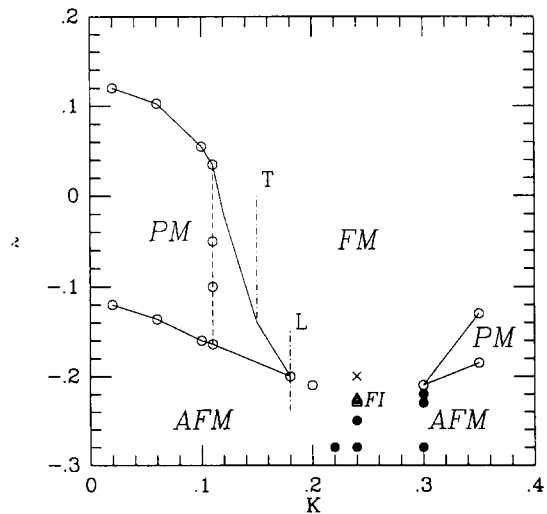


Fig. 2. The same as fig. 1 at  $\lambda=\infty$  and  $(G_\psi=0.1, G_\chi=-1.0)$ . The FI phase is found to exist in a small region in the middle of the  $(K, \kappa)$ -plane, where the FM-PM boundary goes slightly below the PM-AFM boundary. As in fig. 1, we use open circles to represent points in the PM phase. Points in the FM, FI and AFM phases are denoted by crosses, open triangles and full circles, respectively. The dash-dotted line T indicates the range in  $\kappa$  where a systematic scan of the renormalized parameters was performed. The other dash-dotted line L shows the position of the points for fig. 3.

tion of lattice momenta [10]. Our numerical data confirm this behaviour, as shown in fig. 3, where the two scalar masses on the  $4^3 \times 8$  lattice at  $(G_\psi=0.1, G_x=-1.0)$  are displayed along the line L in fig. 2.

Another interesting question is the position of the critical line on which the fermion mass vanishes. Compared to the phase structure at  $(G_\psi=0.1, G_x=-0.3)$ , we find that this line does move out to a slightly larger  $K$  value:  $K_c \approx 0.15$ . This is in accordance with the one-loop prediction. Of course, the one-loop prediction breaks down when Yukawa couplings are strong; therefore, as the couplings are even larger, we have to resort to Monte Carlo simulations. We also notice that at  $(G_\psi=0.1, G_x=-1.0)$  the FI phase starts to show up at some  $K$  value still larger than 0.15 (around  $K=0.21$ ).

The qualitative features of the phase structure do not seem to depend much on the relative magnitude of the two Yukawa couplings. Up to now asymmetric situations with  $|G_\psi| \ll |G_x|$  were discussed, but at  $G_\psi = -G_x$  the situation is quite similar. For instance, at  $G_\psi = -G_x = 2.0$ , we find a similar phase structure as at  $(G_\psi=0.1, G_x=-1.0)$ , but the width of the FI phase gets much wider in the  $\kappa$ -direction, as shown by fig. 4. The width of the FI phase grows as we go to larger values of  $|G_\psi|$  and  $|G_x|$ . Nevertheless, at

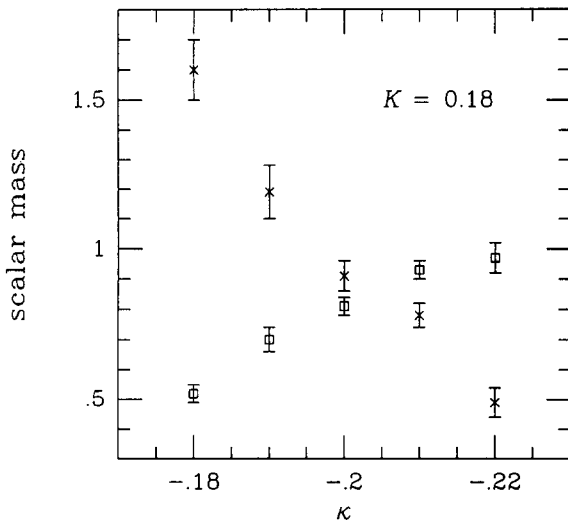


Fig. 3. Mass values for the scalar field  $\phi_x$  (open squares) and for the staggered scalar field  $\hat{\phi}_x$  (crosses) versus  $\kappa$  at  $(K=0.18, G_\psi=0.1, G_x=-1.0)$  in the PM phase, along the line L in fig. 2. It is seen that there is a value for  $\kappa$  where  $m_{R\phi} \approx m_{R\hat{\phi}} \approx 1$ .

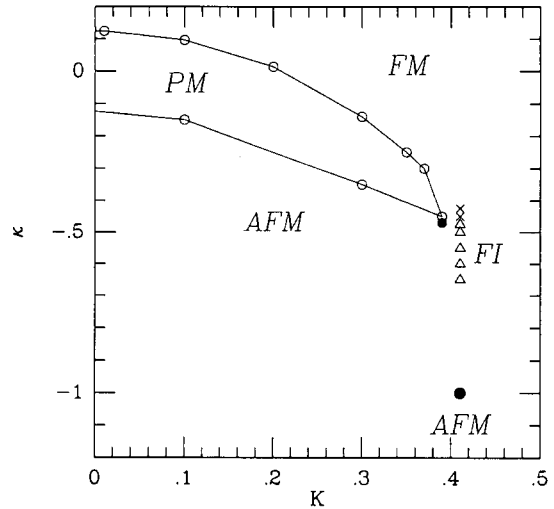


Fig. 4. The phase structure at  $(\lambda=\infty, G_\psi = -G_x = 2.0)$ . For the notation convention of points in different phases see caption of fig. 2. The FI phase is found to exist in a large region at negative  $\kappa$  values.

$G_\psi = -G_x = 2.0$  we observe that for  $\kappa = -1.0$  and  $K = 0.41$  the system is in the AFM phase. This is in agreement with our conjecture: at any fixed values of  $K, G_\psi$  and  $G_x$ , as we move to larger and larger negative  $\kappa$ , the system should at some point go to the AFM phase. That is, the width of the FI phase remains finite. Concerning the behaviour of the fermion mass at  $G_\psi = -G_x = 2.0$  we find that it decreases monotonically as we go to larger values of  $K$ , starting at  $K=0.01$ . At  $K=0.39$ , it is still large, namely around  $\mu_R \approx 2.0$ . This indicates that the critical line on which the fermion mass vanishes passes through the FM, FI and AFM phases. Since for  $G_\psi G_x < 0$  we know that  $K_c$  monotonically increases as  $|G_\psi G_x|$  increases, it is very plausible that at some smaller  $|G_\psi G_x|$  value (a guess is  $G_\psi = -G_x \approx 1.7$ ) the  $K=K_c$  plane will intersect the critical line along which the PM, FM, AFM and FI phases coexist. This intersecting point, which we call  $M_1$ , is an interesting multicritical point of the model. It may be a candidate for a possible non-trivial fixed point.

As we go to even larger  $|G_\psi|$  and  $|G_x|$  at any finite  $K$ , based on the knowledge of the phase structure in the limiting cases, we know that the FI phase will eventually disappear. This FI phase will also vanish if we go to larger and larger  $K$  values at any finite  $G_\psi, G_x$ . What is unknown is the limit where, say, both  $K$

and  $|G_\chi|$  go to infinity with their ratio fixed at some finite value, and  $G_\psi$  is kept finite. In order to treat this limit numerically, one has to remember that up to now the normalization of the fermion field is fixed, according to refs. [3,4], by the  $\psi$ - $\chi$  mixing mass term:  $\bar{\mu} \equiv 1$ . Therefore, if  $|G_\chi| \rightarrow \infty$ , then the ratio  $\bar{\mu}/G_\chi$  is going to zero. In this limit a convenient normalization for the numerical simulations is, say,  $|G_\chi| \equiv 1$ . The other bare fermionic couplings are then:  $\bar{\mu} = G_\psi = 0$  and  $K$  finite. We explored this particular  $|G_\chi| \rightarrow \infty$  limit numerically on a  $4^3 \times 8$  lattice. Here the phase structure is investigated in the  $(K/|G_\chi|, \kappa)$  plane. From the limiting cases mentioned before, we know that at  $K/|G_\chi| = 0, \infty$ , the phase structure is the same as that of the pure scalar model, i.e. the system undergoes a second order phase transition from the FM to PM (PM to AFM) phases at  $\kappa_c \simeq 0.15$  ( $-0.15$ ). What is interesting is the phase structure at intermediate values of  $K/|G_\chi|$ . We want to know whether the FI phase continues to exist there. From our simulations on the  $4^3 \times 8$  lattice, the answer is "yes": the FI phase does exist. This means that in the  $\bar{\mu} = 1$  normalization, as we increase  $|G_\chi|$  indefinitely, the FI phase shifts to larger and larger  $K$  values, and eventually goes to  $K = \infty$  when  $|G_\chi| = \infty$ .

Another interesting question is the position of the critical line where the fermion mass is zero. From our simulations at finite Yukawa couplings, we found that this critical line moves out to larger and larger  $K$  values as we increase  $|G_\chi|$ . Does it go to infinite  $K$  in the  $|G_\chi| \rightarrow \infty$  limit? Starting from  $K/|G_\chi| = 0.02$  we find from our data that the fermion mass monotonically increases as  $K/|G_\chi|$  increases. Therefore  $K_c/|G_\chi| \leq 0.02$ , and it is very likely that  $K_c/|G_\chi| = 0.0$ . This indicates that in the  $\bar{\mu} = 1$  normalization the critical line for zero fermion mass will stay at some finite value of  $K$  and  $|G_\chi| \rightarrow \infty$ . Since the critical point around which the PM, FM, AFM and FI phases in the  $(K, \kappa)$  plane coexist appears to be at finite  $K/|G_\chi|$ , somewhere for large  $|G_\chi|$  it has to cross again the critical surface with zero fermion mass. This second multicritical point, which we call  $M_2$ , is presumably equivalent to  $M_1$ .

In our study of the phase structure, no evidence of a first order phase transition has even been found. All transitions between various phases at the reported Yukawa couplings are consistent with a second order

phase transition. Of course, this statement has to be confirmed on larger lattices.

### 3. Tuning in the broken phase

According to the numerical data the physically interesting broken phase is the FM phase, because in the AFM phase the renormalized Yukawa couplings are always very small, close to zero. Since our important goal is to explore the allowed region of renormalized couplings, we should be able to use our knowledge of the phase diagram in order to suitably tune the bare parameters in the FM phase of the model. For instance, the tuning should be performed in such a way, that the Higgs-scalar mass  $m_R \simeq 1$ , and the renormalized fermion mass  $\mu_R \simeq 0$ . The latter value corresponds to a small renormalized mixing angle  $\alpha_R \simeq 0$  between fermion and mirror fermion (see ref. [4] for the precise definitions). The numerical data show that at  $G_\psi \simeq 0.1$  for  $m_R \simeq 1$ ,  $\mu_R \simeq 0$  the renormalized Yukawa coupling of the fermion (i.e. the ratio of its mass to the renormalized vacuum expectation value) is about  $G_{R\psi} \simeq 0.75$ . As was stated above, the critical value of  $K$  where the fermion mass vanishes does not shift very much in the region of moderately strong  $|G_\chi|$ , and is estimated to be  $K_c \simeq 0.15$  for  $(G_\psi = 0.1, G_\chi = -1.0)$ . In addition to the exploration of the phase diagram, at these values of the Yukawa couplings we performed a systematic scan in the FM phase on a  $4^3 \times 8$  lattice along the critical line at  $K = 0.15$  (see fig. 2), where  $\kappa$  was varied between  $\kappa = -0.05$  and  $-0.12$ . To study the  $K$ -dependence of the renormalized parameters we ran a few more points at neighbouring values of  $K_c$ , namely  $K = 0.14$  and  $K = 0.16$ .

The first observation is that  $G_{R\psi}$  changes from  $G_{R\psi} = 0.5$  at  $K = 0.14$  to  $G_{R\psi} = 1.0$  at  $K = 0.16$  at fixed values of  $\kappa$ . The scan along the critical line at  $K = 0.15$  revealed that  $G_{R\psi}$  is always around 0.75, except for  $\kappa \leq -0.10$  where  $G_{R\psi}$  increases. The scalar mass  $m_R$  turns out to be quite independent of  $\kappa$  along  $K = 0.15$  on the  $4^3 \times 8$  lattice, since  $m_R$  stays around 1.6 as one approaches the critical line of the phase transition to the PM phase. However, the "magnetization" (the vacuum expectation value of the scalar field) is decreasing almost linearly from 0.36 to 0.17 as one goes closer to the critical line, which gives us confidence

that the transition is indeed of second order. The large scalar mass is most likely due to the very small lattice used in the simulation, and hence we repeated the run at  $K=0.15$ ,  $\kappa=-0.10$  on a  $4^3 \times 16$  lattice. There it turns out that the scalar mass is  $m_R \simeq 1.2$ . This shows that the time extension of the  $4^3 \times 8$  lattice is not sufficient to extract the real mass value, even on such a small spatial lattice. Of course, on larger spatial volumes still much smaller Higgs-boson masses can be expected. As was stated in ref. [5], finite size effects on the scalar mass are expected to be rather large in the FM phase. The value for the magnetization in this point on the  $4^3 \times 16$  lattice is  $\langle |\phi| \rangle \simeq 0.185$ .

The scan at  $K=0.15$  shows that for moderate  $|G_\chi|$  the renormalized fermion-mirror-fermion mixing angle  $\alpha_R$  can be tuned to zero, as expected. Once  $\alpha_R$  is fixed, one should vary  $\kappa$  and study the magnetization, in order to tune to an appropriate Higgs-scalar mass in lattice units. It turns out that at the same time the value of the renormalized Yukawa coupling  $G_{R\psi}$  can be kept at a reasonable value around 0.75. Note that taking the physical value of the renormalized vacuum expectation value to be  $v_R \equiv 250$  GeV, this corresponds to a fermion mass of about 190 GeV.

#### 4. Summary

The qualitative phase structure we found in the  $U(1)_L \otimes U(1)_R$  symmetric scalar-fermion model for fixed quartic coupling (here  $\lambda = \infty$ ) at small bare Yukawa couplings in the  $(K, \kappa)$ -plane is shown by the dotted lines in fig. 5. If the Yukawa couplings get stronger this is deformed to the structure shown by the dashed lines: the line of zero scalar mass intersects the curve where the mass of the staggered field is zero in two places. Therefore, in addition to the ferromagnetic (FM), paramagnetic (PM) and anti-ferromagnetic (AFM) phases already present at small bare Yukawa couplings, a fourth phase, namely the ferrimagnetic (FI) phase, appears. The physically interesting broken phase is the FM phase, because in the AFM phase the renormalized Yukawa couplings are zero. The lines  $Z, Z'$  in fig. 5 represent the critical lines corresponding to zero fermion mass  $\mu_R = 0$ . Note that those curves are no phase boundaries.

The qualitative picture of the phases does not seem to depend strongly on the ratio  $G_\psi/G_\chi$  of the bare

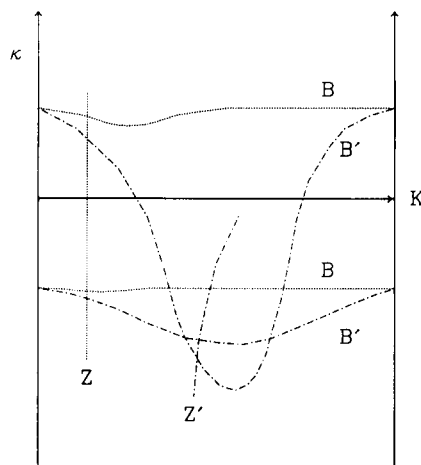


Fig. 5. The schematic behaviour of the phase boundaries at small (dotted lines with label B) and large (dashed lines with label B') bare Yukawa couplings in the  $(K, \kappa)$ -plane for fixed  $\lambda$ . The lines  $Z, Z'$  represent the curves of zero fermion mixing mass for small and large Yukawa couplings, respectively.

Yukawa couplings of fermion and mirror fermion. This means that, for instance, the case  $G_\psi = -G_\chi$  with a degenerate fermion-mirror-fermion pair is not much different from an asymmetric situation  $|G_\psi/G_\chi| \ll 1$ , which in the FM phase, due to the large mirror fermion mass, comes closest to the situation in the minimal standard model.

Since in the FM phase one often wants to tune to  $\mu_R = 0$ , which corresponds to no mixing among fermion and mirror fermion, it is interesting to ask for the phase structure in the subspace defined by  $\mu_R = 0$ . This is qualitatively shown in fig. 6. In fact, in most other numerical simulations up to now [6-13] the bare fermion mass was fixed at zero, therefore the comparison is best done by fig. 6. In this figure there are four phases (FM, PM, AFM and FI), but the PM phase is split into two parts ( $PM_1$  and  $PM_2$ ). In our case, however, the two parts are connected to each other in the full parameter space. The spectrum is in both parts qualitatively the same, and the fermion masses are by definition zero both in  $PM_1$  and  $PM_2$ . This is different from the PMW and PMS phases found in the Smit-Swift model [9], because there the fermion spectrum is not the same [17]. The problem is that in the Smit-Swift model not all renormalizable (mass dimension  $\leq 4$ ) terms are included in the action, which would be possible in terms of elemen-

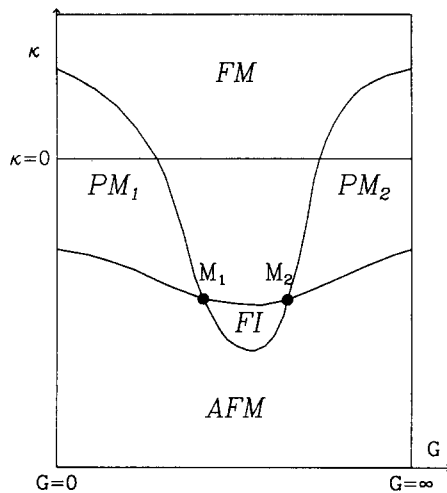


Fig. 6. The result of cutting the phase structure in fig. 5 by the zero fermion mass critical lines, shown as a function of the scalar hopping parameter  $\kappa$  and some bare Yukawa coupling, here  $G \equiv -G_x$ . In this subspace the PM phase has two parts:  $PM_1$  and  $PM_2$ . At  $\lambda = \infty$ ,  $G_y = 0.1$  we find the point  $M_1$  around  $-G_x \approx 1.0-1.5$ ,  $-\kappa \approx 0.2-0.3$ .

tary fields with the quantum numbers of the fermion spectrum present in the PMS phase. In an appropriately enlarged parameter space the fermion masses could presumably be tuned to zero also there, and our PM phase with two parts ( $PM_1$  and  $PM_2$ ) could eventually be found. In some other models, where the required elementary fermion fields are present in the action, the addition and tuning of a fermion mass term should be enough.

Since the two parts of the PM phase in fig. 6 are equivalent, most probably the two multicritical points  $M_1$  and  $M_2$  are also equivalent. As suggested by the scalar propagator found in ref. [10], and supported by our data in fig. 3, at these multicritical points the continuum limit contains two scalar degrees of freedom. Since in the whole of fig. 6  $\mu_R = 0$  by definition, the continuum limit contains also the fermions and mirror fermions. Future studies should answer the questions about the behaviour of the couplings near the multicritical points  $M_1$ ,  $M_2$ . These points are the best candidates for possibly non-trivial fixed points. Nevertheless, one has to note that  $M_1$  and  $M_2$  are in regions of the parameter space, where reflection positivity of the lattice action could not be proven [4]. Furthermore, since the scalar spectrum is enlarged by a second state, not all renormalizable couplings of the

corresponding fields are explicitly included in the lattice action. The study of renormalization of the couplings near  $M_1$  and  $M_2$  may require the introduction of such new bare parameters.

If one considers continuum limits at the boundary of the  $FM-PM_1$  or  $FM-PM_2$  phases, but not at the multicritical points  $M_1$  or  $M_2$ , then the low mass spectrum corresponds to the fields in the action (a single scalar plus fermions and mirror fermions). In order to be safe about reflection positivity, one can stay at  $\kappa \geq 0$ , where link-reflection positivity can be proven for any couplings [4]. In section 3 it was shown how the parameters can be tuned in the FM phase for such continuum limits. By using this information the numerical determination of the allowed region for the renormalized couplings, between the upper and lower limits for the renormalized quartic scalar coupling, should be possible.

#### Acknowledgement

We thank Gernot Münster for active help and useful discussions. The Monte Carlo calculations for this paper have been performed on the CRAY Y-MP of HLRZ, Jülich.

#### References

- [1] I. Montvay, Phys. Lett. B 199 (1987) 89.
- [2] L. Lin, J.P. Ma and I. Montvay, Z. Phys. C 48 (1990) 355.
- [3] K. Farakos, G. Koutsoumbas, L. Lin, J.P. Ma, I. Montvay and G. Münster, Nucl. Phys. B 350 (1991) 474.
- [4] L. Lin, I. Montvay, G. Münster and H. Wittig, Nucl. Phys. B 355 (1991) 511.
- [5] L. Lin, I. Montvay, G. Münster, H. Wittig, DESY preprint 90-142, Nucl. Phys. B (Proc. Suppl.), to be published.
- [6] D. Stephenson and A. Thornton, Phys. Lett. B 212 (1988) 479;  
A. Thornton, Phys. Lett. B 214 (1988) 577; B 221 (1989) 151.
- [7] A. Hasenfratz and T. Neuhaus, Phys. Lett. B 220 (1989) 435;  
A. Hasenfratz, W. Liu and T. Neuhaus, Phys. Lett. B 236 (1990) 339;  
J. Berlin, A. Hasenfratz, U.M. Heller and M. Klomfass, Phys. Lett. B 249 (1990) 485.
- [8] I.-H. Lee, J. Shigemitsu and R. Shrock, Nucl. Phys. B 330 (1990) 225; B 334 (1990) 265;  
S. Aoki, I.-H. Lee, J. Shigemitsu and R.E. Shrock, Phys. Lett. B 243 (1990) 403;  
S. Aoki, I.-H. Lee, D. Mustaki, J. Shigemitsu and R.E. Shrock, Phys. Lett. B 244 (1990) 301.

- [9] W. Bock, A.K. De, K. Jansen, J. Jersák and T. Neuhaus, Phys. Lett. B 231 (1989) 283;  
W. Bock, A.K. De, K. Jansen, J. Jersák, T. Neuhaus and J. Smit, Nucl. Phys. B 344 (1990) 207;  
W. Bock and A.K. De, Phys. Lett. B 245 (1990) 207.
- [10] K. Jansen, Proc. Intern. Conf. on Lattice field theory, Lattice 90 (Tallahassee, FL, 1990), Nucl. Phys. B (Proc. Suppl.) 20 (1991) 564.
- [11] M.A. Stefanov and M.M. Tsypin, Phys. Lett. B 236 (1990) 344; B 242 (1990) 432; Oxford preprint OUTP-90-47P.
- [12] S. Sanielevici, H. Gausterer, M.F.L. Golterman and D.N. Petcher, FSU-SCRI preprint 90C-183 (1990).
- [13] J. Berlin and U.M. Heller, FSU-SCRI preprint 90C-186 (1990).
- [14] J. Shigemitsu and M.F.L. Golterman, lectures at Intern. Conf. on Lattice field theory, Lattice 90 (Tallahassee, FL, 1990), Nucl. Phys. B (Proc. Suppl.) 20 (1991) 515.
- [15] M.J. Duncan, R. Philippe and M. Sher, Phys. Lett. B 153 (1985) 165;  
M. Lindner, Z. Phys. C 31 (1986) 295;  
M. Sher and H.W. Zaglauer, Phys. Lett. B 206 (1988) 537;  
M. Sher, Phys. Rep. 179 (1989) 273;  
M. Lindner, M. Sher and H.W. Zaglauer, Phys. Lett. B 228 (1989) 139.
- [16] S. Duane, A.D. Kennedy, B.J. Pendleton and D. Roweth, Phys. Lett. B 195 (1987) 216.
- [17] A.K. De, Proc. Intern. Conf. on Lattice field theory, Lattice 90 (Tallahassee, FL, 1990), Nucl. Phys. B (Proc. Suppl.) 20 (1991) 572.